remote sensing

MDPI

Article

Joint Optimization of Data Transmission and Energy Harvesting in Relay Satellite Networks

Jun Long [1,2], Ying Wan [1,3], Lin Guo [1,2,*], Limin Liu [1] and Rui Ding [1]

[1] School of Computer Science and Engineering, Central South University, Changsha 410075, China; junlong@csu.edu.cn (J.L.); yingwan@csu.edu.cn (Y.W.); liulimin@csu.edu.cn (L.L.); dingrui666@csu.edu.cn (R.D.)
[2] Big Data Institute, Central South University, Changsha 410075, China
[3] School of Information Science and Engineering, Hunan Women's University, Changsha 410012, China
* Correspondence: guolincsu@csu.edu.cn

Abstract: Satellite network is considered a prominent architecture for future space-air-ground integrated networks, where the relay satellite network (RSN) plays an essential role in data transmission. However, the relay satellite network faces practical challenges. First, due to the dynamic network topology and limited resources such as storage capacity, antennas, and bandwidth, optimizing data transmission and resource allocation in a resource-constrained stochastic system is challenging. Second, satellites intermittently enter the eclipse zone, which leads to an unstable energy supply. Therefore, optimal energy management is required to balance energy supply and consumption. In this paper, we proposed an online optimal control algorithm, based on Lyapunov stability theory, to optimize data transmission and energy management jointly. Furthermore, the performance of our proposal is analyzed comprehensively, including the reasonable bounds for data and energy and the optimality of our proposed algorithm. Finally, extensive performance evaluation simulations are performed based on real-world satellite parameters. The simulation results indicate that the proposed method can achieve long-term network stability and energy sustainability. Moreover, the proposed algorithm shows an improvement of 9.6% and 20.3% in system utility compared to the non-optimized transmission method and non-optimized energy management algorithm, respectively.

Keywords: relay satellite network; data transmission; resource allocation; stochastic optimization

Citation: Long, J.; Wan, Y.; Guo, L.; Liu, L.; Ding, R. Joint Optimization of Data Transmission and Energy Harvesting in Relay Satellite Networks. *Remote Sens.* **2023**, *15*, 2629. https://doi.org/10.3390/rs15102629

Academic Editor: Salvatore Stramondo

Received: 26 February 2023
Revised: 4 May 2023
Accepted: 16 May 2023
Published: 18 May 2023

1. Introduction

With the rapid development of spatial information networks (SIN), space-air-ground integrated networks (SAGIN) have received extensive attention in recent years [1]. In many application scenarios, such as resource exploration and environment monitoring, the terrestrial networks cannot be deployed due to topographical reasons [2]. Acting as a backbone architecture in SIN, the satellite network can efficiently transfer the data randomly generated in these special scenarios due to its wide coverage and high communication capacity [3]. In view of the small size and low cost, low earth orbit (LEO) satellites can be deployed in large numbers to collect high-quality data from the earth. However, some types of LEO satellites (e.g., remote sensing satellites, meteorological satellites) are not networked in satellite cluster [4]. These satellites can only download the on-board data for a few minutes when they are within the coverage of ground stations [5], which brings significant challenges in downloading spatial data. To tackle the data transmission problem, the relay satellite network (RSN) is considered a prominent solution. In RSN, geostationary earth orbit (GEO) satellites are dedicated to supplying data forwarding services for user satellites (i.e., LEO satellites) through the seamless switching of inter-satellite links (ISLs) [6]. In addition, GEO satellites with stable orbits can download received data to ground stations via satellite-ground links (SGLs).

It is of paramount importance to design reliable and stable transmission strategies for the stochastic arrived data in RSN. Different from the terrestrial network with static properties, the topology of RSN changes dynamically due to the periodic operation of user satellites in their own orbits. Furthermore, limited resources of RSN (e.g., battery capacity, transmission bandwidth, and transceivers) may complicate the data transmission decisions. Generally, solar energy harvesting has been utilized to power LEO satellites [7]. However, the LEO satellites harvest energy only when exposed to the sun. The satellite is mainly in a discharging state during the eclipse phase [8], which further limits the data acquisition and transmission. Moreover, only background knowledge about dynamic network topology, channel transmission capacity, and solar exposure duration is available. This may pose great challenges in stable transmission and sustainable energy supply over the whole network operation process. This can be manifested in the following two aspects:

- **Random data arrivals and fluctuating energy supply.** First, spatial data arrives at user satellites randomly, which leads to the data buffer varying over time. A larger data cache will prolong the transmission time due to limited network capacity, which may result in transmission delay. Second, the remaining battery capacity fluctuates dynamically due to the energy consumption required for data acquisition and transmission [9]. Furthermore, satellite networks face dynamic energy supply due to unstable illumination. Each satellite charges itself by receiving solar energy only when the satellites move to the sunny side. Particularly, the satellite may fall to a resting state due to insufficient residual energy, which would decrease transmission performance [10]. Thus, an optimization control method with sustainable energy is required to transmit the stochastic arrived data.
- **Time-variant inter-satellite link.** Due to the intermittent connection between GEO satellites and LEO satellites, ISLs have time-varying characteristics. Although potential ISLs are predictable, technical research on inter-satellite routing is required to enhance transmission performance [11]. In addition, the number of antennas that can be used to establish ISLs is limited, which will directly affect the transmission state of satellites [12]. This challenges the resource allocation and link contact plan design (CPD). On the one hand, if the LEO satellite connected to the GEO satellite has insufficient energy to achieve transmission, it will cause a waste of antenna resources. On the other hand, the connected user satellites with a small data buffer will waste scarce bandwidth resources. Therefore, it is of vital importance to develop effective link allocation strategies in dynamic satellite networks.

In the literature, there have been some data transmission scheduling schemes for satellite networks [13,14]. These methods improve the transmission performance to a certain extent, but ignore the impact of insufficient energy supply for satellites in practical applications. Motivated by the actual problems considered in this paper, there are also some works on designing joint energy and resource allocation strategies [15,16]. However, these works are mainly oriented to predictable data arrival, which cannot be applied to the scheduling of stochastic arrived data directly. The existing works [17,18] on data transmission with random data arrival has more or less some limitations, such as operating in a finite-horizon or requiring prior statistics on data arrivals. Therefore, an energy-efficiently collaborative transmission method should be carefully designed for random arrived data.

To comprehensively consider the characteristics of the relay satellite network, we systematically study an online data transmission optimization method, which can achieve a higher system utility and long-term stability. The main contributions of this paper can be summarized as follows:

- We design a dynamic stochastic system model considering the RSN features (i.e., dynamics of network topology, limited transmission resources, and unstable energy supply). We present a multi-objective optimization problem to maximize system utility without prior statistics knowledge about the stochastic process.

- To solve the joint optimization problem of data transmission and energy management in stochastic satellite networks, we propose an online optimal control algorithm, named DTEM, which can improve transmission performance and energy efficiency. In particular, we construct an optimization framework based on Lyapunov stability theory to decompose the optimization problem into three sub-problems, i.e., data acquisition, energy harvesting, and inter-satellite transmission. Based on this, our proposed method can adaptively optimize the system variables (i.e., data acquisition rate, energy harvesting rate, ISL contact state, and transmission rate) at each time slot.
- We analyze the performance of our proposed algorithm in satellite networks comprehensively, including the maximum storage of buffer and the minimum capacity of the battery, which are required to maintain system stability. Furthermore, we compare the time-average system optimal performance with the global system optimal solution. Further, we establish a satellite scenario under dynamic network topology and conduct extensive simulations to demonstrate the efficiency of our method.

The remainder of this paper is structured as follows. In Section 2, we introduce the related work about data transmission schemes in satellite networks. In Section 3, we design a dynamic stochastic system model and summarize our optimization formula for maximizing system utility. In Section 4, we elaborate on the solution strategy and propose an efficient online algorithm, and the analysis for system performance is discussed in Section 5. Then, extensive simulations are illustrated in Section 6. Finally, this paper is concluded in Section 7.

2. Related Work

As we know, the research about data transmission schemes in satellite networks has been intensively studied. Mainly, RSN relays space data from LEO satellites at the user satellite layer to ground stations directly, which attracts many researchers to improve network transmission performance.

In the literature, there have been some data transmission scheduling schemes for executing tasks with predictable data arrival [16,19,20]. In [16], a two-stage task scheduling scheme has been designed, which decomposes task scheduling into a power allocation (PA) problem and a PA-based task scheduling optimal problem. The authors in [19] presented a task scheduling algorithm composed of two stages, i.e., an initial scheduling stage and a dynamic scheduling stage. In [20], a heuristic mission scheduling algorithm has been given, in which the dynamic setting of antennas based on visibility window constraints is considered. To solve the problem of scheduling hybrid tasks, a stochastic optimization framework has been proposed [21], which can maximize the average time of tasks by joint optimization of the scheduling period and antenna allocation. The authors in [22] suggested a task scheduling schema considering breakpoint transmission. In the scheme, a single task is split into multiple sub-tasks and rationally arranged in multiple transmission time windows.

Some existing efforts have studied resource optimization strategies in data transmission [23–25]. To schedule stochastic arrived data, wang et al. proposed a queue stability model and a dynamic contact capacity optimization scheme [23]. An et al. [24] considered different strategies, to obtain optimal power and adaptive transmission rate in a relay satellite network. In [25], the authors designed a resource optimization model to realize the continuity of radio resources for mapping with packets. In addition, several studies explore reinforcement learning methods to address the resource allocation problem. In [26], the authors focused on power allocation, power splitting, and time allocation optimization strategies corresponding to the static and dynamic schemes. To optimize relay and transmission power resources, a deep Q-network-based approach is proposed in underwater acoustic sensor networks with energy harvesting module [27]. Chen et al. [28] studied the optimization of resource utilization and proposed a Markov decision process algorithm considering the energy status of the relay nodes. The authors in [29] utilize a deep rein-

forcement learning model to improve the effectiveness of computational task offloading in SAGIN.

For the time-varying dynamic topology of satellite networks, the ISLs between satellites are not persistent, which exhibits the characteristics of a delay tolerant network (DTN) [30,31]. To make effective use of limited network resources, some works focus on routing (i.e., link allocation) in the literature, such as [32,33]. Limited by the number of transceivers, Zhou et al. obtained the maximum feasible contacts between satellites based on conflict graphs (CGs) with the same edge weight [18]. To avoid a large-scale routing table caused by calculating all routes, the authors in [34] proposed a routing calculation schema based on contact graph routing (CGR), employing four strategies. To overcome the problem that CGR is limited in large-capacity transmission, Zhang et al. designed a multi-flow maximizing routing strategy based on a storage time aggregation graph (STAG) [35]. To send the same information to multiple users, the authors proposed an energy-efficient routing scheme with a delay guarantee based on the multicast time-expanded graph (MTEG) [36]. In [37], D.Raverta et al. exploited uncertain contact plans to enhance data transmission under which routing is described as the Markov Decision Process (MDP) with multiple copies.

To summarize, most of the current data transmission strategies are geared towards predictable data transfer tasks or do not fully consider the impact of energy harvesting on network performance. For practical application in time-varying satellite networks, the data transmission scheme should consider optimization of the data acquisition rate, link allocation, inter-satellite transmission rate, and energy harvesting. Although reinforcement learning can cope with the dynamics and complexity of satellite systems, such methods require extensive training to learn optimization strategies. In this paper, we work on an online optimal control method for energy-efficient data transmission that does not require the prior knowledge.

3. System Model and Problem Formulation

In this section, we design a stochastic system model that includes the RSN network, dynamic models of data queue, and energy queue. Then, a system utility maximization problem is formulated with multiple constraints. The key notations with descriptions used in this paper are summarized in Table 1.

Table 1. Notations description.

Symbol	Description
U	Set of user satellites
R	Set of relay satellites
T	Set of time slots
$\mathcal{D}_i(t)$	Data queue of user satellite i in slot t
$\delta_{ij}(t)$	Connection state of ISL in slot t
$\xi_{ij}(t)$	ISL capacity in slot t
$\varphi_i(t)$	Data acquisition rate of user satellite i in slot t
$\gamma_i(t)$	Inter-satellite transfer rate of user satellite i in slot t
$\rho_i(t)$	Energy Harvesting rate of user satellite i in slot t
$E_i^c(t)$	Energy consumption at user satellite i in slot t
$E_i^h(t)$	Harvested energy at user satellite i in slot t
$E_i(t)$	Energy queue of user satellite i in slot t

3.1. Network Model

The relay satellite network considered in this paper consists of four parts: a set of user satellites denoted as $i \in U = \{1, 2, \ldots, M\}$ that are moving on their low orbits, geosynchronous relay satellites $j \in R = \{1, 2, \ldots, N\}$, ground stations $G = \{1, 2, \ldots, L\}$ and data management center (DMC). Consider a typical time-slotted RSN that operates over T time slots presented as $t \in \mathcal{T} = \{0, 1, 2, \ldots, T\}$, and the interval of the slot is τ. As shown

in Figure 1, the user satellite collects data from the earth or space environment and stored it in the buffer. The relay satellite provides forwarding service for user satellites with intermittent ISLs and then downloads the received data to ground stations via continuous SGLs (i.e., DMC) directly. Here, we set a binary variable $\delta_{ij}(t)$ to indicate whether user satellite i is connected to relay satellite j or not at time slot t. When $\delta_{ij}(t) = 1$, the user satellite transmits spatial data to the relay satellite, otherwise, $\delta_{ij}(t) = 0$.

In particular, each relay satellite employs K antennas, which can establish ISLs with up to K user satellites simultaneously. Additionally, a user satellite can only connect to one relay satellite due to the limited antenna. For example, when $K = 1$, if the i-th user satellite establishes a connection with the j-th relay satellite at time slot t, then the relay satellite j cannot provide forwarding services for other user satellites at that slot. We have the following formulas:

$$\sum_{j=1}^{N} \delta_{ij}(t) \leq 1, \qquad \forall i \in U. \tag{1}$$

$$\sum_{i=1}^{M} \delta_{ij}(t) \leq K, \qquad \forall j \in R. \tag{2}$$

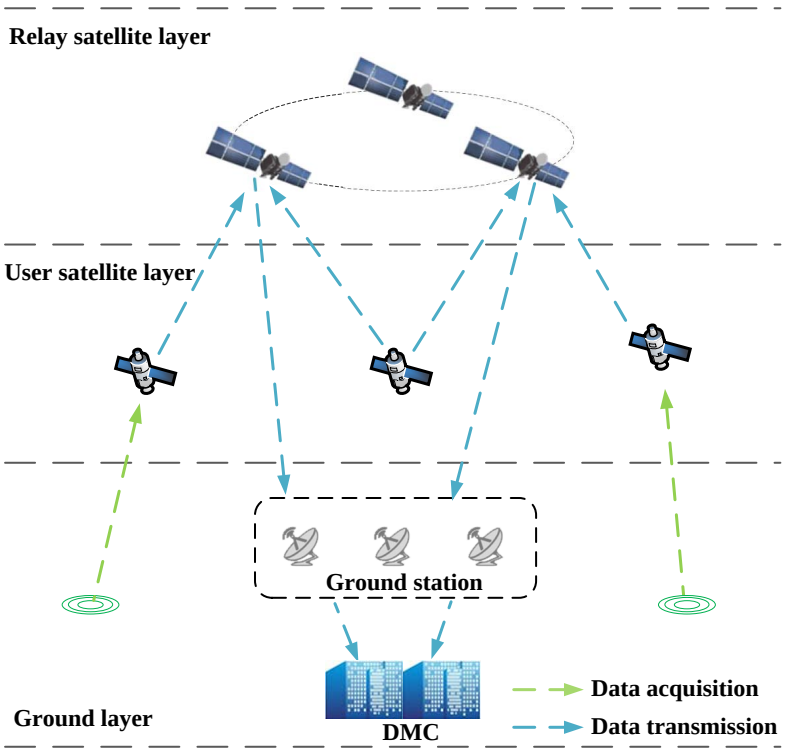

Figure 1. RSNs architecture.

3.2. Transmission Model and Data Queue

In RSN, different user satellites have different types of data acquisition missions. Considering the differentiated data amount of missions, we denote $\varphi_i(t)$ as the data collection rate of user satellite i in slot t. The upper bound of $\varphi_i(t)$ is denoted by $\varphi_{\max}$, i.e.,

$$0 \leq \varphi_i(t) \leq \varphi_{\max}. \tag{3}$$

The spatial data collected by the user satellite at each time slot is first stored in the buffer and then transmitted in a carry-forward mode. We define $\mathcal{D}_i(t)$ as the buffered data

queue length at the beginning of slot t. We also let $\xi_{ij}(t)$ be the link capacity from user satellite i to relay satellite j [38], expressed by

$$\xi_i(t) = \frac{P_u G_t G_r L_s(t) L_f}{kT_s \cdot (E_b/N_0)_{\text{req}} \cdot M_a}, \tag{4}$$

where P_u is the ISL transmission power (in W). G_t is the transmitting antenna gain of the user satellite. G_r is the receiving antenna gain of the relay satellite. $L_s(t)$ and L_f are the free space loss and the total line loss, respectively. k is the Boltzmann's constant (in JK^{-1}), and M_a is the link margin. Furthermore, T_s is the temperature of system noise (in K), and $(E_b/N_0)_{\text{req}}$ is the ratio of received energy per bit to noise density. We define $\xi_{\max}$ as the upper bound of link capacity, i.e., $\xi_i(t) \leq \xi_{\max}$.

In addition, we define $\gamma_i(t)$ as the inter-satellite transmission rate of satellite i through ISL in slot t, which is limited by the link capacity. Therefore, we have

$$0 \leq \gamma_i(t) \leq \xi_i(t). \tag{5}$$

We formulate the data queue evolution of user satellite i by input process and delivery process, which corresponds to data acquisition rate $\varphi_i(t)$ and data transfer rate $\gamma_i(t)$, i.e.,

$$\mathcal{D}_i(t+1) = [\mathcal{D}_i(t) - \tau \sum_{j=1}^{N} \delta_{ij}(t)\gamma_i(t)]^+ + \tau\varphi_i(t), \tag{6}$$

where $\tau\varphi_i(t)$ is the data flow entering data buffer in slot t, and $\tau \sum_{j=1}^{N} \delta_{ij}(t)\gamma_i(t)$ is the data flow leaving data queue in time slot t, respectively. To keep the stability of the data queue, we impose the following constraint that the total collected data is less than the transferred data over the infinite time horizon, i.e.,

$$\lim_{T\to+\infty} \frac{1}{T} \sum_{t=0}^{T-1} \sum_{i=1}^{M} \varphi_i(t) \leq \lim_{T\to+\infty} \frac{1}{T} \sum_{t=0}^{T-1} \sum_{i=1}^{M} \sum_{j=1}^{N} \delta_{ij}(t)\gamma_i(t). \tag{7}$$

3.3. Energy Consumption and Harvesting Model

In RSNs, the energy management of user satellites consists of two parts: energy consumption and energy harvesting. The three factors that affect energy consumption are the satellite's orbital movement, data acquisition, and transmission. Denote E_i^c as energy consumption of user satellite i in slot t, which is given by

$$E_i^c(t) = \tau \times \left(P_n + P_t \cdot \frac{\gamma_i(t)}{\xi_{\max}} \cdot \delta_{ij}(t) + P_r \cdot \frac{\varphi_i(t)}{\varphi_{\max}} \right). \tag{8}$$

Wherein, P_n, P_t, and P_r are the constant power of regular operation, data transmission, and data acquisition, respectively. Since the data collection rate $\varphi_i(t)$ has a maximum value of $\varphi_{\max}$ and the inter-satellite transmission rate $\gamma_i(t)$ is with the maximum value of $\xi_{\max}$. We derive the upper bound of total energy consumption as $E_{\max}^c = \tau \cdot (P_n + P_t + P_r)$.

Since a satellite moves around the earth, it harvests energy when the satellite runs to the sunny side. Denote E_i^h as the amount of energy harvested by satellite i ($i \in U$) during slot t as follows

$$E_i^h(t) = \rho_i(t) \times \max\{0, \tau - \omega_i(t)\}, \tag{9}$$

where $\omega_i(t)$ is the remaining time of user satellite i in the shadow during time slot t, and $\omega_i(t) = 0$ implies satellite i is in eclipse. The energy harvesting rate $\rho_i(t)$ is bounded by $\rho_{\max}$.

In the dynamic process of energy, buffered energy $E_i(t+1)$ at user satellite i is related to $E_i(t)$, consumed power, and harvested energy in slot t. We build the time-varying energy queue model as follows

$$E_i(t+1) = E_i(t) - E_i^c(t) + E_i^h(t). \tag{10}$$

Normally, the remaining energy in the battery at the end of time slot t is bound by its maximum capacity. In addition, the battery needs to retain a certain amount of energy to ensure the regular operation of the satellite. Thus, we have the following constraint

$$\mathcal{B}(1-\mu) \leq E_i(t) \leq \mathcal{B}, \qquad \forall i \in U, \tag{11}$$

where $\mathcal{B}$ denotes the capacity of the satellite battery, and μ represents the maximum energy consumption proportion of the battery.

3.4. Problem Formulation

According to (7), it is clear that the total data arriving at the network affects the throughput of the satellite network. Thus, optimizing the data acquisition rate can enhance the network transmission capacity while avoiding congestion and achieving system stability. On this basis, we give the objective function, which maximizes the time-average system utility (MTASU), as

$$\begin{aligned} &\text{MTASU}: \max_{\Theta(\mathrm{t})} \lim_{\mathrm{T}\to\infty} \frac{1}{\mathrm{T}} \sum_{\mathrm{t}=0}^{\mathrm{T}} \mathbb{E}[\mathcal{H}(\mathrm{t})] \\ &s.t.\ \textit{feasible contact constraints}: \ (1)\text{–}(2); \\ &\quad \textit{data transmission constraints}: \ (3)\text{–}(7); \\ &\quad \textit{energy management constraints}: \ (8)\text{–}(11). \end{aligned}$$

Wherein $\mathcal{H}(t) = U[\varphi_i(t)] = \sum_{i=1}^{\mathrm{M}} \log\,(1+\varphi_i(t))$ is the system utility. $\Theta(t)$ is defined as the set of vectors in slot t, including ISL contact state, data acquisition rate, inter-satellite transmission rate, energy consumption, and energy harvesting, which can be written as $\Theta(t) = (\delta_{ij}(t), \varphi_i(t), \gamma_i(t), E_i^c(t), E_i^h(t))$.

4. Solutions and Algorithms

In this section, we propose a decomposition strategy to solve the MTASU problem using the Lyapunov optimization method. Then, we devise an online algorithm, named DTEM, to obtain optimum solutions without prior statistics knowledge about the stochastic variables (i.e., ISL contact state, data acquisition rate, transmission rate, and energy harvesting rate on user satellites) for any time slot.

4.1. Solution Development

As mentioned above, MTASU is a multi-objective mixed-integer optimization (MMO) problem with integer and continuous parameters, which is difficult to tackle. Furthermore, RSN is a stochastic network with time-varying uncertainties. We solve the MMO problem based on the Lyapunov optimization framework.

4.1.1. Lyapunov Function

First, we define $L(t)$ as the Lyapunov function to describe the square of all modeled queues in time slot t, i.e.,

$$L(t) = \frac{1}{2} \sum_{i=1}^{M} \left[\mathcal{D}_i^2(t) + (E_i(t) - \mathcal{B})^2 \right], \tag{12}$$

where $(E_i(t) - \mathcal{B})$ denotes the remaining capacity of the battery.

4.1.2. Lyapunov Drift

To maintain the stability of RSN, we define a Lyapunov drift function $\Delta(t)$ to describe the difference of the Lyapunov function between two adjacent time slots, with the following expression

$$\Delta(t) = \mathbb{E}[L(t+1) - L(t)|\Pi(t)], \tag{13}$$

where $\Pi(t)$ is system state at slot t with the expression of $\Pi(t) \triangleq (\mathcal{D}(t), E(t))$. By minimizing $\Delta(t)$, the queues $\mathcal{D}_i$ and $E_i(t)$ can approach a stable state over the operation process.

4.1.3. Collaborate System Utility

An improved Lyapunov Drift function $\Delta_V(t)$ is defined by collaborating system utility $\mathcal{H}(t)$, expressed as

$$\Delta_V(t) = \mathbb{E}[\Delta(t) - V\mathcal{H}(t)|\Pi(t)], \tag{14}$$

where V is a positive constant to tradeoff system utility and stability. Compared with the Lyapunov drift function, minimizing $\Delta_V(t)$ can simultaneously maximize system utility and achieve system stability.

Since it is not easy to obtain the minimum value of $\Delta_V(t)$ directly, we turn to minimize the maximum of $\Delta_V(t)$ as obtained in Theorem 1.

Theorem 1. *Under the condition of modeled queues and system utility $\mathcal{H}(t)$, the maximum value of $\Delta_V(t)$ is expressed by*

$$\Delta_V(t) \leq \mathbb{E}[\Gamma_V(t)|\Pi(t)] + \Lambda, \tag{15}$$

where Λ is a constant that can be denoted as

$$\Lambda = \frac{M}{2}\left[(\tau\xi_{\max})^2 + (\tau\varphi_{\max})^2 + (\tau\rho_{\max})^2 + (E^c_{\max})^2\right]. \tag{16}$$

As shown in (17), $\Gamma_V(t)$ is a function of the variables in $\Pi(t)$ and the process of proof is expressed in Appendix A.

$$\begin{aligned}\Gamma_V(t) = &\underbrace{\sum_{i=1}^{M}\rho_i(t)(\tau-\omega_i(t))(E_i(t)-\mathcal{B})}_{\text{BMO}}\\ &+\underbrace{\sum_{i=1}^{M}\tau\left[\mathcal{D}_i(t)-\frac{P_r}{\varphi_{\max}}(E_i(t)-\mathcal{B})\right]\varphi_i(t) - V\mathcal{H}(t)}_{\text{DACO}}\\ &+\underbrace{\sum_{i=1}^{M}\sum_{j=1}^{N}\tau\left[\frac{P_t}{\xi_{\max}}(\mathcal{B}-E_i(t))-\mathcal{D}_i(t)\right]\delta_{ij}(t)\gamma_i(t)}_{\text{LTO}}.\end{aligned} \tag{17}$$

Since Λ is a constant, $\Delta_V(t)$ can be minimized by minimizing $\Gamma_V(t)$. According to the system stochastic variables, $\Gamma_V(t)$ is divided into three parts in (17). Thus, we can achieve the initial optimization goal by optimizing the energy harvesting rate $\rho_i(t)$, data acquisition rate $\varphi_i(t)$, ISL contact plan $\delta_{ij}(t)$, and inter-satellite transmission rate $\gamma_i(t)$.

4.2. Decomposition Strategy

As shown in (17), we transform the optimization problem of minimizing $\Gamma_V(t)$ to three sub-problems: battery management optimization (BMO), data acquisition control optimization (DACO), and link transmission optimization (LTO), which are optimized separately.

4.2.1. Battery Management

For the optimization of the BMO problem, we aim at minimizing the first part in (17), i.e.,

$$\text{BMO}: \min_{\rho_i(t)} \sum_{i=1}^{M} \rho_i(t)(\tau - \omega_i(t))(E_i(t) - \mathcal{B})$$
$$s.t.\ (9),\ (11).$$

According to constraint (11), we have $E_i(t) - \mathcal{B} \leq 0$, and $\tau - \omega_i(t)$ is a constant in each time slot due to the periodic motion of the celestial bodies. Note that it is pointless to optimize $\rho_i(t)$ when the satellite is in shadow during time slot t. Thus, the optimal solution can be obtained by maximizing energy harvest rate $\rho_i(t)$ when $0 < \tau - \omega_i(t)$. In other words, the RSN should harvest energy from the sun as much as possible until the battery capacity is full. The optimal solution $\rho_i^*(t)$ can be obtained as follows

$$\rho_i^*(t) = \min\{(\mathcal{B} - E_i(t))/(\tau - \omega_i(t)), \rho_i(t)\}. \tag{18}$$

4.2.2. Data Acquisition Control

For the DACO problem, we need to minimize the second part in (17) under the constraint of (3), i.e.,

$$\text{DACO}: \min_{\varphi_i(t)} \sum_{i=1}^{M} \tau\left[\mathcal{D}_i(t) - \frac{P_r}{\varphi_{\max}}(E_i(t) - \mathcal{B})\right]\varphi_i(t) - V\mathcal{H}(t)$$
$$s.t.\ (3).$$

Note that $\mathcal{H}(t)$ is a concave function of $\varphi_i(t)$, and the other part of DACO is linear. Therefore, the DACO problem is convex, which can be solved based on the convex optimization theory. Denote $\varphi_i^*(t)$ as the optimal solution of DACO, we have

$$\varphi_i^*(t) = \begin{cases} \varphi_{\max}, & \varphi_{\max} \leq F_L, \\ F_L, & 0 < F_L < \varphi_{\max}, \\ 0, & others, \end{cases} \tag{19}$$

where $F_L = (V\varphi_{\max})/(\tau D_i(t)\varphi_{\max} - \tau P_r(E_i(t) - \mathcal{B})) - 1$.

4.2.3. Data Transmission and Link Allocation

To solve the link transmission and link allocation problem, we should minimize the third part in (17) under corresponding constraints as follows

$$\text{LTO}: \min_{\delta_{ij}(t),\gamma_i(t)} \sum_{i=1}^{M}\sum_{j=1}^{N} \tau\left[\frac{P_t}{\xi_{\max}}(\mathcal{B} - E_i(t)) - \mathcal{D}_i(t)\right]\delta_{ij}(t)\gamma_i(t)$$
$$s.t.\ (1), (2), (5).$$

Note that the ISL contact state $\delta_{ij}(t)$ and the transmission rate $\gamma_i(t)$ are integer variable and continuous variable, respectively. It is easy to know the LTO problem is a mixed-integer linear programming (MILP) problem, which is proved to be an NP-hard problem. Thus, we solve the LTO problem in steps. To express our solution conveniently, let $\delta_{ij}^*(t)$ and $\gamma_i^*(t)$ be the optimal ISL contact state and transmission rate, respectively. Moreover, $\lambda_i(t)$ is defined as the weight of LTO at slot t, i.e.,

$$\lambda_i(t) = \frac{P_t}{\xi_{\max}}(\mathcal{B} - E_i(t)) - \mathcal{D}_i(t). \tag{20}$$

Before the ISL is established, satellites are constantly harvesting energy and collecting space data. In this case, the energy queue $E_i(t)$ continues to approach the capacity of

battery $\mathcal{B}$, and the data queue $\mathcal{D}_i(t)$ keeps approaching the maximum storage of buffer. According to constraint (11), we have

$$\lambda_i(t) < 0. \tag{21}$$

Thus, we can obtain the solution for LTO by maximizing $\delta_{ij}(t) \cdot \gamma_i(t)$. There is no need to optimize the transmission rate when the ISL contact is inactive, i.e., $\delta_{ij}(t) = 0$. It makes sense to optimize the transmission rate when $\delta_{ij}(t) = 1$. Thus, we can obtain the optimal ISL contact state as follows

$$\delta_{ij}^*(t) = 1. \tag{22}$$

In order to improve system utility, the RSN should transfer data to the relay satellite as much as possible when the ISL contact is active. Note that the inter-satellite transmission rate is limited by link capacity. Thus, link capacity is the optimal solution for transmission rate, i.e.,

$$\gamma_i^*(t) = \xi_i(t). \tag{23}$$

In addition, the transmission rate can reach the optimal solution only when $\mathcal{D}_i(t)$ is larger than ISL capacity. Therefore, the necessary condition of Formula (23) is $\mathcal{D}_i(t) \geq \xi_i(t)$. To this end, the LTO problem can be transformed into a link allocation optimization (LAO) problem, expressed as

$$\begin{aligned} \text{LAO}: \min_{\delta_{ij}(t)} & \sum_{i=1}^{M} \sum_{j=1}^{N} \tau \lambda_i(t) \delta_{ij}(t) \xi_i(t) \\ s.t. \ & (1), (2). \end{aligned}$$

To minimize $\lambda_i(t)$, relay satellites tend to assign antennas to user satellites with longer data queues and energy queues. We can observe that the LAO problem falls in the category of a weighted maximum matching problem. As shown in Figure 2, the link allocation problem can be represented as a weighted bipartite graph (WBG). Let M be the user satellite set and N be the relay satellite set. For each $i \in M$, $j \in N$, we denote w_{ij} as the weight of edge from i to j. According to (20), we set $w_{ij} = \mathcal{D}_i(t) - \frac{P_t}{\xi_{\max}}(\mathcal{B} - E_i(t))$. Then, the LAO problem can be effectively addressed based on the WBG by the Kuhn–Munkres (KM) algorithm [39].

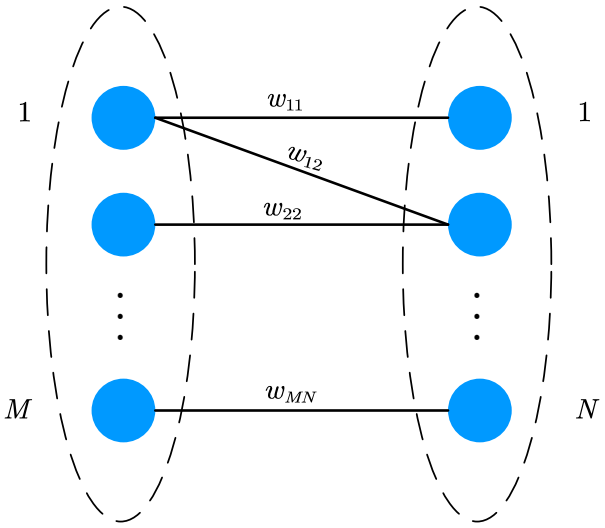

Figure 2. Weighted bipartite graph: the transformed link assignment.

4.3. Algorithm Design

As shown in Algorithm 1, an online data transmission and energy management (DTEM) method is proposed to obtain optimal solutions for energy-efficient data transmis-

sion problems. The designed algorithm consists of four steps. Firstly, we can obtain the optimal solution for the EHO problem (lines 1–5). Secondly, the solution for the DACO problem is proposed to obtain an optimal data acquisition rate (lines 6–13). Then, we formulate a many-to-many matching problem to solve the problem of link allocation (line 14). Based on this, we can obtain the optimal solution for the LTO problem (lines 15–19). Finally, the data queue $\mathcal{D}_i(t+1)$ and energy queue $E_i(t+1)$ are calculated based on the obtained optimal solutions, i.e., $\rho_i^*(t)$, $\varphi_i^*(t)$, $\delta_{ij}^*(t)$ and $\gamma_i^*(t)$ (lines 20–22).

Algorithm 1: DTEM

Input : $\mathcal{D}_i(t), E_i(t), \forall i \in M$.
Output: $\rho^*(t), \varphi^*(t), \delta_{ij}^*(t), \gamma_i^*(t), \mathcal{D}(t+1), E(t+1)$.

`/* Solution for the EHO problem */`
1 **for** $i \in M$ **do**
2 **if** $\rho_i(t)(\tau - \omega_i(t)) \leq \mathcal{B} - E_i(t)$ **then**
3 $\rho_i^*(t) = \rho_i(t)$.
4 **else**
5 $\rho_i^*(t) = (\mathcal{B} - E_i(t))/(\tau - \omega_i(t))$.

`/* Solution for the DACO problem */`
6 **for** $i \in M$ **do**
7 $F_L = (V\varphi_{\max})/(\tau D_i(t)\varphi_{\max} - \tau P_r(E_i(t) - \mathcal{B})) - 1$.
8 **if** $F_L \geq \varphi_{\max}$ **then**
9 $\varphi_i^*(t) = \varphi_{\max}$.
10 **else if** $F_L \leq 0$ **then**
11 $\varphi_i^*(t) = 0$.
12 **else**
13 $\varphi_i^*(t) = F_L$.

`/* Solution for the LTO problem */`
14 Solve the LAO problem to obtain $\delta_{ij}^*(t)$.
15 **for** $i \in M$ **do**
16 **if** $\sum_{j=1}^{N} \delta_{ij}(t) == 1$ **then**
17 $\gamma_i^*(t) = \xi_i(t)$.
18 **else**
19 $\gamma_i^*(t) = 0$.

`/* Update data queue and energy queue */`
20 **for** $i \in M$ **do**
21 Compute $\mathcal{D}_i(t+1)$ according to (6).
22 Compute $E_i(t+1)$ according to (8).

We analyze the time complexity of the DTEM algorithm including three parts, i.e., EMO, DACO, and LTO. Since the problems EMO and DACO are independent for each user satellite and can be solved by distributed computing. Therefore, the time complexity of the LTO problem can be regarded as that of DTEM, which is determined by the KM algorithm. Hence, the complexity of the DTEM algorithm is to solve the KM algorithm in the worst case, i.e., $O((\max[K * N, M])^3)$.

5. Performance Analysis

In this section, we give the performance analysis of the DTEM algorithm and system stability. Specifically, the maximum storage of buffer, minimum capacity of the battery, and the gap between the optimality of DTEM and optimal system utility are derived, respectively.

5.1. Maximum Storage of Buffer

Since ISL has the characteristic of intermittent connection, data overflow can be solved by a large buffer.

Theorem 2. *Assume the data queue satisfies Formula (24) for any $V > 0$ at $t = 0$, that is*

$$0 \leq \mathcal{D}_i(0) \leq (1/\tau)V\mathcal{H}'_{\max} + \tau\varphi_{\max}, \quad \forall i \in U \tag{24}$$

where $\mathcal{H}'_{\max}$ is the maximum value of the first order derivative of system utility $\mathcal{H}(t)$, and the maximum of data queue $\mathcal{D}_{\max} = (1/\tau)V\mathcal{H}'_{\max} + \tau\varphi_{\max}$. Thus, we have

$$0 \leq \mathcal{D}_i(t) \leq (1/\tau)V\mathcal{H}'_{\max} + \tau\varphi_{\max}, \quad \forall i \in U, t \in \mathcal{T} \tag{25}$$

Proof of Theorem 2. See Appendix B. □

From (25), we can observe that the maximum data storage of each user satellite increases with the maximum data sampling rate. As defined in the optimization objective function (**MTASU**), a larger sampling rate brings a larger system utility, which indicates that increasing the system utility requires more storage capacity to ensure the system stability.

5.2. Minimum Capacity of Battery

In RSN, the satellite should work at the best performance with the support of enough battery capacity. Thus, the minimum capacity of the battery is derived to ensure the performance of RSN by considering that the satellite cannot transmit data due to lack of energy, i.e., $E_i(t) \leq E^c_{\max}$. For the LTO problem, it is in the case that the ISL is not active, i.e., $\delta_{ij}(t) = 0$. Thus, we have $\lambda_i(t) \geq 0$, which is contrary to (21). The appropriate size of $\mathcal{B}$ for the energy queue is shown in Theorem 3.

Theorem 3. *Only and if only the residual energy cannot support the maximum energy consumption, i.e., $E_i(t) \leq E^c_{\max}$, the battery capacity of satellite i can be defined as*

$$\mathcal{B} = E^c_{\max} + \mathcal{D}_{\max}\frac{\xi_{\max}}{P_t}, \quad i \in U. \tag{26}$$

Proof of Theorem 3. See Appendix C. □

As shown in (26), the required battery capacity $\mathcal{B}$ is related to the maximum data storage size $\mathcal{D}_{\max}$ of each satellite. The larger $\mathcal{D}_{\max}$, the larger $\mathcal{B}$ will be. This indicates that a larger battery capacity is required to provide sustainable energy to transmit the increased data backlog.

5.3. Optimization Performance

In Theorem 4, we give the analysis of the optimization performance for DTEM, which shows the gap of system utility between DTEM and the optimal solution.

Theorem 4. *The time-average system utility of DTEM is denoted as $\overline{\mathcal{H}}$ and the optimal system utility as $\mathcal{H}^*$. We have*

$$\overline{\mathcal{H}} \geq \mathcal{H}^* - \frac{B}{V} \tag{27}$$

Proof of Theorem 4. See Appendix D. Theorem 4 shows that the gap of optimality is within $\mathcal{O}(1/V)$ for $\overline{Q}$ and Q^*. According to (27), the system utility $\overline{Q}$ will approach the optimal system utility Q^* by increasing V. □

6. Simulation Evaluation

6.1. Simulation Setup

We build an RSN scenario based on the Satellite Toolkit (STK) which can provide real-world satellite parameters such as orbit inclination and altitude. Then, we evaluate the proposed DTEM algorithm by using the MATLAB simulator. Specifically, the RSN scenario consists of twenty LEO satellites (i.e., user satellites), three GEO satellites, and six GSs. The user satellites are distributed in four orbits with five satellites for each. The orbital altitudes are set to 816 km with an inclination of 86.58°. We assume that one relay satellite is equipped with three antennas, i.e., $K = 3$, and each relay satellite is allocated two ground stations. The network operation period is set to one day which is divided into 1440 time slots, i.e., the slot duration τ is 60 s. We obtain the network topology and sunlight time windows of user satellites for all time slots from the Satellite Toolkit (STK). The ISL transmission capacity randomly takes a value between [8, 10] Mbps, and the maximum data acquisition rate is $\varphi_{\max} = 30$ Mbps. The parameters of energy management are set as follows: $P_n = 10$ W, $P_t = 20$ W, $P_r = 25$ W, $\mu = 80\%$ [15]. Furthermore, we set the maximum energy harvesting rate as $\rho_{\max} = 50$ W with probability 0.8 or $(1/3)\rho_{\max}$ with probability 0.2 when the RSN expose to the sun. Initially, we set $\mathcal{D}_i(0) = 0$ and $E_i(0) = \mathcal{B}$, respectively, where $\mathcal{B}$ is derived from (26).

6.2. System Utility

We evaluate the effects of weights V on system utility as shown in Figure 3. As we can see, with the increase in V, the system utility follows an upward trend. It verifies the theory that a larger V can increase the system utility as Theorem 4. It can be further noted that the system utility increases rapidly at the initial stage. Since system utility $\mathcal{H}(t)$ is a concave function, it can be observed that the growth rate of $\mathcal{H}(t)$ decreases when $V > 2 \times 10^5$.

To test the performance of the proposed DTEM algorithm in improving system utility, four benchmark algorithms are taken for comparison. We evaluate the effectiveness of different optimization modules (i.e., data transmission and energy management) separately. In terms of the data transmission performance, we compare the DTEM algorithm with a fair contact plan (FCP) scheme proposed in [40], which allocates ISL connections with maximum cumulative disable connection opportunities. We also set a Random Link Matching Scheme (RLMS) via the idea of ISL allocation in [18] for comparison. In terms of the energy management performance, we consider two reference schemes, a greedy algorithm [41] with maximum remaining energy (GMR) for ISL contacts and an energy harvesting for the randomness scheme (EHRS) [23]. Specifically, FCP and RLMS have a similar control strategy for energy harvesting and data acquisition as DTEM, but without a data transfer optimization module. Correspondingly, GMR and EHRS do not consider energy management optimization compared to DTEM.

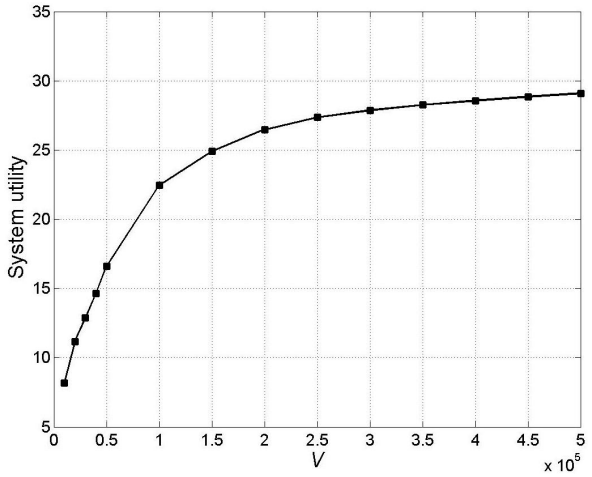

Figure 3. System utility versus V.

The system utility of DTEM and benchmark algorithms are compared under different weights V in Figure 4, where we can observe that DTEM has the highest system utility among the three algorithms. As mentioned in Section 4, the optimal solution for the DACO problem indicates that a smaller size of the data queue or a larger size of the energy queue will result in a higher data acquisition rate (i.e., system utility). Since the DTEM schema jointly optimizes the performance of data transmission and energy harvesting, DTEM is superior to the other four schemes in improving system utility. It can be observed that the system utility increases with the weight V at the beginning and converge afterwards in Figure 4. The reason is that V is a weight to tradeoff the system utility and stability. According to (14), a larger V brings a larger system utility. Furthermore, since $U(t)$ is a logarithm, the increase in system utility slows down after $V > 2 \times 10^5$.

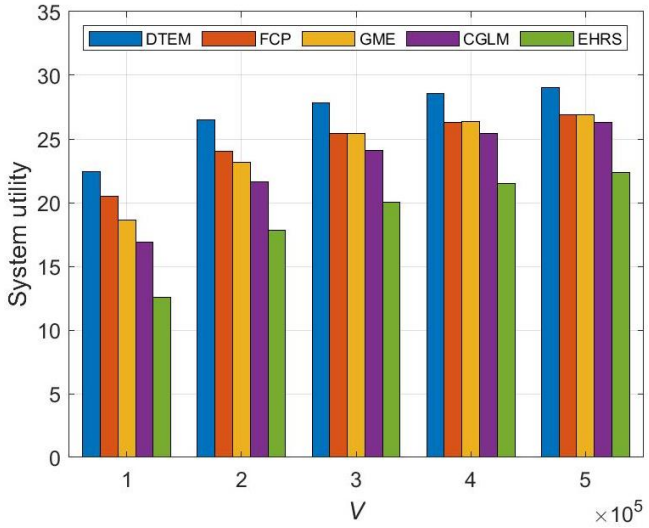

Figure 4. System utility comparison under different V.

To further test the performance of DTEM, the system utility of all five algorithms has been evaluated under different numbers of antennas on relay satellites (i.e., K) and different maximum data acquisition rates $\varphi_{\max}$, respectively. We can observe that DTEM can achieve higher system utility compared with benchmark algorithms under different K in Figure 5. Furthermore, the system utility increases with the increase in antenna number, which enables more data transmission to relay satellites. Then, the system utility trends stable level due to the bottleneck of limited energy harvested by user satellites. Figure 6 depicts the system utility of DTEM and benchmark algorithms under different $\varphi_{\max}$. It can be shown that DTEM has better performance gain in system utility than the other four schemes. Moreover, the increase in $\varphi_{\max}$ can bring higher system utility. However, when the maximum data acquisition rate rises to some value, the system utility is improved very slowly. This is due to the limited transmission channels and energy resources. In terms of the maximum system utility, DTEM has a performance improvement of 4.8%, 9.6%, 10.6%, and 20.3% compared to FCP, CGLM, GME, and EHRS, respectively, when the maximum data acquisition rate $\varphi_{\max} = 100$ Mbps. This is attributed to the joint optimization of data transmission scheduling and energy management.

6.3. Queue Length and Queue Dynamics

In Figures 7 and 8, we show the relationship between time-averaged queue length and weights V. It can be noted that the maximum storage buffer and battery capacity increases linearly with the value of V, which is derived in Theorems 2 and 3. As expected, the time-averaged length of $E_i(t)$ and $\mathcal{D}_i(t)$ keeps linearly increasing with V, which matches with the theoretical analysis in Equations (25) and (A4).

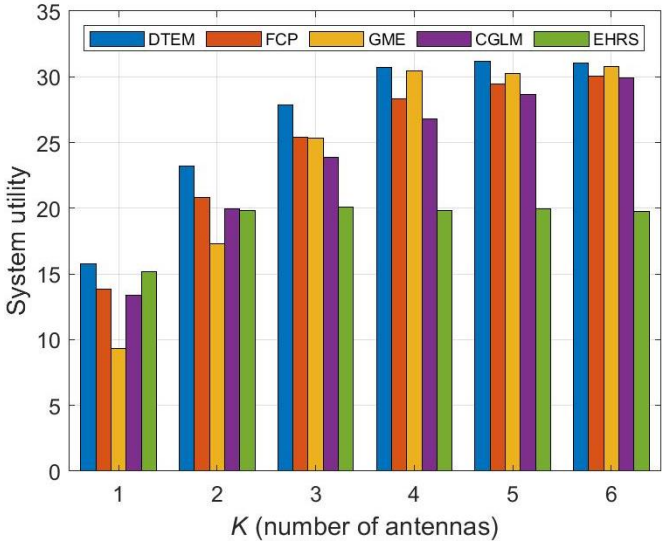

Figure 5. System utility comparison under different K.

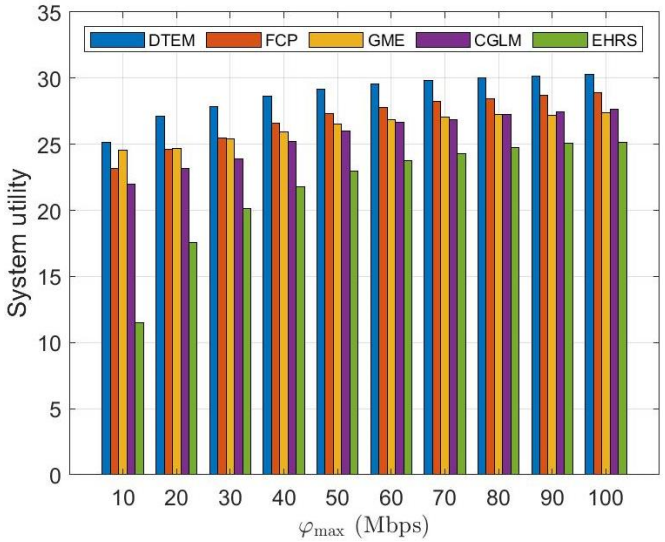

Figure 6. System utility comparison under different $\varphi_{\max}$.

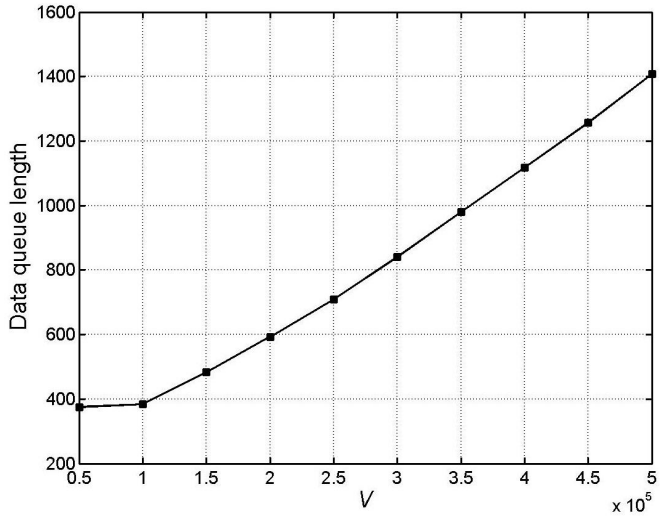

Figure 7. Time-averaged data queue length versus V.

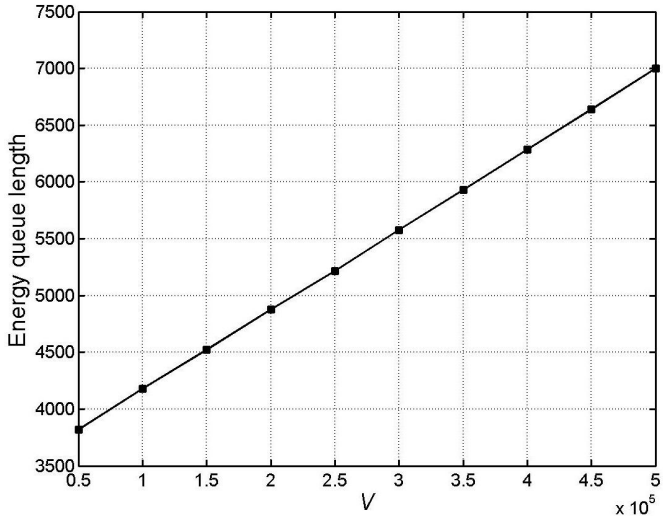

Figure 8. Time-averaged energy queue length versus V.

In order to demonstrate the stability of the RSN under the DTEM scheme, we evaluate the dynamic processes for $\mathcal{D}_i(t)$ over 1440 time slots with different V. As shown in Figure 9, $\mathcal{D}_i(t)$ rises sharply at the initial stage, then decreases slowly and fluctuates around a certain value. The reason lies in that no data is stored in the queue, which allows satellites to collect spatial data as much as possible. Subsequently, the collected data is transmitted to relay satellites through ISL. During the operation of RSN, our proposed online DTEM algorithm controls data acquisition and transmission in a dynamic balance state. In addition, a larger weight V brings a longer data queue. This implies that a larger V requires a larger storage buffer to guarantee network stability.

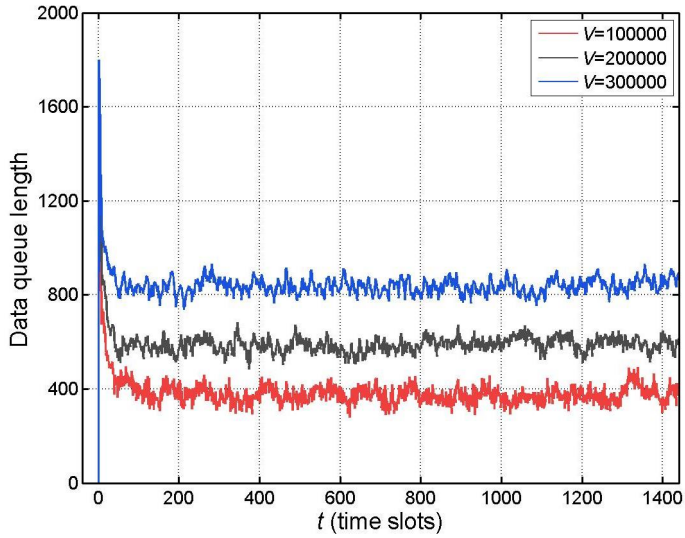

Figure 9. The dynamics of data queue with different V.

Figure 10 presents the dynamic processes for $E_i(t)$ over 1440 time slots with different V. We can observe that $E_i(t)$ reaches a large value at $t = 0$. With the operation of the system, the length of the energy queue decreases and quickly converges to a relatively stable state. This is because the energy queue length is initialized to the size of maximum battery capacity according to Equation (26). In addition, the battery management model of DTEM is effective for energy consumption and harvesting, which makes the energy queue achieve a dynamic balance. Although satellites harvest solar energy as much as possible when they move to the sunny side, there is only energy consumption when satellites are eclipsed by the earth. As a result, $E_i(t)$ cannot always be reached the full battery capacity.

Similar to the reasons shown in Figure 9, a larger V requires the RSN to carry a larger battery capacity to ensure the sustainability of the network.

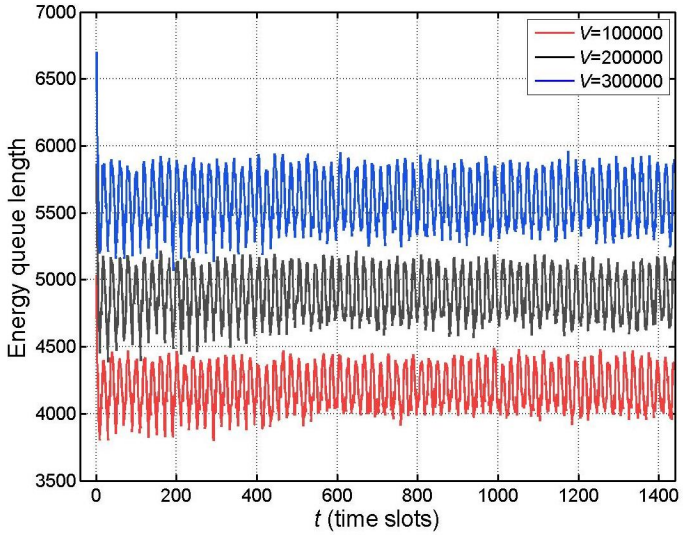

Figure 10. The dynamics of energy queue with different V.

6.4. Impact of System Parameters

In Figures 11 and 12, we explore the impacts of system parameters on DTEM regarding antennas number equipped at relay satellites and the maximum data acquisition rate of user satellites.

In Figure 11, we evaluate the effect of antenna number on system utility. It can be observed that the system utility increases as the number of antennas K increases under different three weights V. This can be explained by the fact that an increase in K implies an increase in the number of transmission channels which can improve transmission capacity. Accordingly, the network will achieve a higher system utility. Moreover, we can observe that the increasing trend of system utility stops for a certain value of K due to the bottleneck of the harvested energy at user satellites.

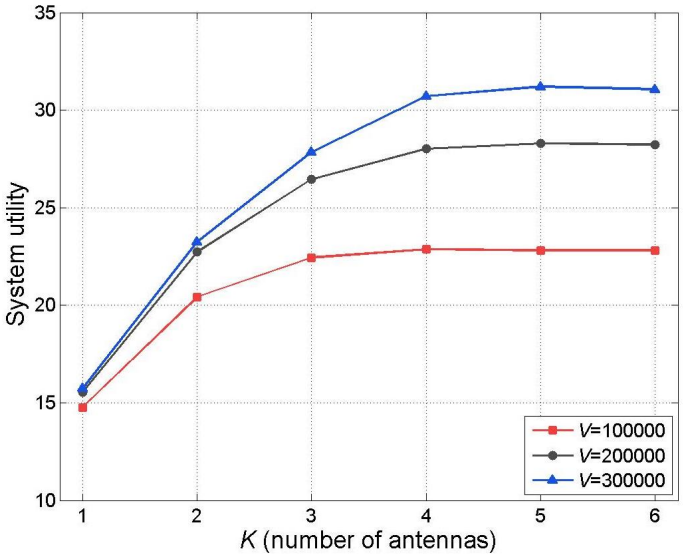

Figure 11. The utility of RSNs versus K.

Figure 12 reveals the impact of parameter $\varphi_{\max}$ (i.e., the maximum data acquisition rate of user satellites) on system utility. From the figure, we can see that the system utility of DTEM increases with the increase in $\varphi_{\max}$, which corresponds to the definition of system

utility. However, as $\varphi_{\max}$ further increases, the system utility increases very slowly under different three weights V. This is because the transmission capacity and energy resources of user satellites become the bottleneck.

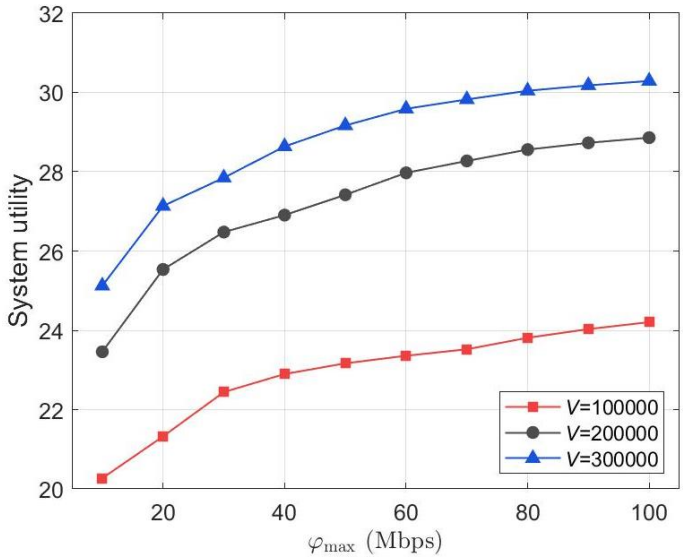

Figure 12. The utility of RSNs versus $\varphi_{\max}$.

7. Conclusions

In this paper, considering the stochastic network state and random data arrivals demand, we formulated the data transmission scheduling problem with a joint resource allocation and ISL assignment as a system utility optimization problem. We proposed the DTEM algorithm, based on the Lyapunov stability theory, to enhance system utility and guarantee system stability. To reduce computational complexity, we decompose the optimization problem into battery management optimization, data acquisition control optimization, and inter-satellite transmission optimization. Then, we solved the three sub-problems to obtain the optimal energy harvesting rate, data acquisition rate, inter-satellite transmission rate, and ISL connection allocation for each time slot. Moreover, the system performance is analyzed comprehensively. Finally, extensive simulation results show the superiority of DTEM in improving system utility and maintaining long-term network stability and sustainability. Specifically, our proposed algorithm shows an improvement of 9.6% in system utility compared to the non-optimized transmission method and 20.3% compared to the non-optimized energy-management approach, respectively.

Author Contributions: Conceptualization, J.L. and Y.W.; methodology, Y.W. and L.G.; software, Y.W., L.L. and R.D.; formal analysis, J.L., L.L. and R.D.; writing—original draft preparation, Y.W.; writing—review and editing, J.L. and L.G.; supervision, L.L.; funding acquisition, J.L., Y.W. and L.G. All authors have read and agreed to the published version of the manuscript.

Funding: This work was supported in part by the National Natural Science Foundation of China (Nos. 62102456, U2003208, 61972398, and 62202501), in part by the Foundation of Preview of Equipment (No. 6141A020227), in part by Theory and Method of Multi-Satellite Collaborative Application (No. 2019-JCJQ-ZD-342-00), in part by the Project funded by China Postdoctoral Science Foundation (No. 2021TQ0369), in part by a Project Supported by Scientific Research Fund of Hunan Provincial Education Department (No. 22B0922), in part by National Key R&D Program of China (No. 2021YFB3900902), and in part by the Science and Technology Plan of Hunan (Nos. 2016TP1003 and 2022JJ40638).

Data Availability Statement: Data in this study are available upon request by contacting the corresponding author.

Conflicts of Interest: The authors of this current research declare that this study has no competing interest.

Appendix A. Proof of Theorem 1

We square Formulas (6) and (7), respectively, to obtain the following Equations (A1) and (A2), i.e.,

$$\begin{aligned}\mathcal{D}_i^2(t+1) =& \Big[\mathcal{D}_i(t) - \sum_{j=1}^{N}\delta_{ij}(t)\gamma_i(t)\tau\Big]^2 + \varphi_i^2(t)\tau^2 + 2\Big[\mathcal{D}_i(t) - \sum_{j=1}^{N}\delta_{ij}(t)\gamma_i(t)\tau\Big]^+\varphi_i(t)\tau \\ \leq& \mathcal{D}_i^2(t) + \sum_{j=1}^{N}\delta_{ij}^2(t)\gamma_i^2(t)\tau^2 + \varphi_i^2(t)\tau^2 - 2\mathcal{D}_i(t)\sum_{j=1}^{N}\delta_{ij}(t)\gamma_i(t)\tau + 2\mathcal{D}_i(t)\varphi_i(t)\tau \\ \leq& (\tau\xi_{\max})^2 + (\tau\varphi_{\max})^2 + \mathcal{D}_i^2(t) + 2\tau\mathcal{D}_i(t)\Big(\varphi_i(t) - \sum_{j=1}^{N}\delta_{ij}(t)\gamma_i(t)\Big)\end{aligned} \tag{A1}$$

$$\begin{aligned}\big(E_i(t+1)-\mathcal{B}\big)^2 =& \big((E_i(t)-\mathcal{B}) - E_i^c(t) + E_i^h(t)\big)^2 \\ \leq& (E_i(t)-\mathcal{B})^2 + \big(E_i^c(t)\big)^2 + \big(E_i^h(t)\big)^2 + 2(E_i(t)-\mathcal{B})\big(E_i^h(t) - E_i^c(t)\big) \\ \leq& (\tau\rho_{\max})^2 + (E_{\max}^c)^2 + (E_i(t)-\mathcal{B})^2 + 2(E_i(t)-\mathcal{B})\big(E_i^h(t) - E_i^c(t)\big)\end{aligned} \tag{A2}$$

Then, according to (11) and (12), we can derive the following formula

$$\begin{aligned}\Delta(t) =& \frac{1}{2}\sum_{i=1}^{M}\left[\mathcal{D}_i^2(t+1) + (E_i(t+1)-\mathcal{B})^2 - \mathcal{D}_i^2(t) - (E_i(t)-\mathcal{B})^2\right] \\ \leq& \frac{M}{2}\Big[(\tau\xi_{\max})^2 + (\tau\varphi_{\max})^2 + (\tau\rho_{\max})^2 + (E_{\max}^c)^2\Big] + (E_i(t)-\mathcal{B})\big(E_i^h(t) - E_i^c(t)\big) \\ &+ \sum_{i=1}^{M}\Big[\tau\mathcal{D}_i(t)\Big(\varphi_i(t) - \sum_{j=1}^{N}\delta_{ij}(t)\gamma_i(t)\Big)\Big]\end{aligned} \tag{A3}$$

Appendix B. Proof of Theorem 2

Since $\mathcal{D}_i(0)$ satisfies the constraint of data queue upper-bound, Theorem 2 can be proved by mathematical induction. Assume that $0 \leq \mathcal{D}_i(t) \leq \mathcal{D}_{\max}$ holds in time slot t. According to (6), we have $0 \leq \mathcal{D}_i(t+1)$. Then, we focus on proving Formula (25) holds at time slot $t+1$, i.e., $\mathcal{D}_i(t+1) \leq \mathcal{D}_{\max}$.

(1) If $\varphi_i(t) = 0$ at time slot t, no data is collected by satellite i. We have $\mathcal{D}_i(t+1) \leq \mathcal{D}_i(t) \leq \mathcal{D}_{\max}$.

(2) If satellite i collected space data in time slot t, i.e., $\varphi_i(t) \geq 0$. Note that the DACO problem is a convex problem, we have $(1/\tau)V\mathcal{H}'(\varphi_i^*(t)) = \mathcal{D}_i(t) - (P_r/\varphi_{\max})(E_i(t)-\mathcal{B})$. Since $E_i(t) - \mathcal{B} \leq 0$ and $\mathcal{H}'(\varphi_i^*(t)) \leq \mathcal{H}'_{\max}$, we have $\mathcal{D}_i(t) \leq (1/\tau)V\mathcal{H}'_{\max}$. According to (6), we can obtain $\mathcal{D}_i(t+1) \leq \mathcal{D}_i(t) + \tau\varphi_i(t)$. Therefore, we have $\mathcal{D}_i(t+1) \leq (1/\tau)V\mathcal{H}'_{\max} + \tau\varphi_{\max}$.

Appendix C. Proof of Theorem 3

The battery capacity $\mathcal{B}$ is derived when the residual energy of satellite i is insufficient for data transmission and ISL is inactive, i.e., $E_i(t) \leq E_{\max}^c$ and $\delta_{ij}(t) = 0$. Thus, we have $(P_t/\xi_{\max})(\mathcal{B} - E_i(t)) - \mathcal{D}_i(t) \leq 0$ when $\delta_{ij}(t) = 0$, i.e.,

$$\mathcal{B} \leq E_i(t) + \mathcal{D}_i(t)\frac{\xi_{\max}}{P_t}. \tag{A4}$$

To ensure the ISL cannot be established when $E_i(t) \leq E_{\max}^c$, we maximize $\mathcal{D}_i(t)$ in (A4). Then, we have

$$\mathcal{B} = E_{\max}^c + \mathcal{D}_{\max}\frac{\xi_{\max}}{P_t}. \tag{A5}$$

Appendix D. Proof of Theorem 4

Denote a random algorithm as Θ. We prove the optimality of the DTEM algorithm by comparing $\Delta_V(t)$ with the algorithm Θ. Furthermore, variables generated by each algorithm will be tagged by DTEM and Θ, respectively. According to the Lyapunov optimization theory proposed by Neely [42], the upper bounds of algorithm Θ are as follows,

$$\begin{cases} \mathbb{E}\left[\sum\limits_{n\in\mathcal{N}} U(\varphi_i^{\Theta}(t))\right] & \leq \mathcal{H}^* + \zeta, \\ \left|\mathbb{E}\left[\sum\limits_{n\in\mathcal{N}}\left(\varphi_i^{\Theta}(t) - \sum\limits_{j=1}^{N}\delta_{ij}^{\Theta}(t)\gamma_i^{\Theta}(t)\right)\right]\right| & \leq \eta_1\zeta, \\ \left|\mathbb{E}\left[\sum\limits_{n\in\mathcal{N}}\left((E_i^h)^{\Theta}(t) - (E_i^c)^{\Theta}(t)\right)\right]\right| & \leq \eta_2\zeta, \end{cases} \tag{A6}$$

where ζ is positive and infinitesimal, and η_1, η_2 are constants.

According to (12) and (A6), we minimize $\Delta_V(t)$ in (14) and have

$$\begin{aligned} \Delta(t) - V\mathcal{H}(t) &\leq \mathbb{E}\left[\Gamma_V^{DTEM}(t)|\Pi(t)\right] + B \\ &\leq \mathbb{E}\left[\Gamma_V^{\Theta}(t)\right] + B \\ &\leq (\eta_1 + \eta_2 + 1)\zeta - V\mathcal{H}^* + B. \end{aligned} \tag{A7}$$

Then, by setting ζ to a minimum value, (A7) can be simplified to

$$\Delta(t) - V\mathcal{H}(t) \leq B - V\mathcal{H}^*. \tag{A8}$$

Take the expectation (A8), (A8) can be deduced as

$$\frac{1}{T}(L(T-1) - L(0)) - \frac{1}{T}\sum_{t=0}^{T-1}\mathbb{E}[\mathcal{H}(t)] \leq B - V\mathcal{H}^*. \tag{A9}$$

Since $L(t)$ is finite, by $T \to \infty$, we have $\overline{\mathcal{H}} \geq \mathcal{H}^* - B/V$.

References

1. Lyu, F.; Wu, F.; Zhang, Y.; Xin, J.; Zhu, X. Virtualized and Micro Services Provisioning in Space-Air-Ground Integrated Networks. *IEEE Wirel. Commun.* **2020**, *27*, 68–74. [CrossRef]
2. Aranda, L.A.; Reviriego, P.; Maestro, J.A. Toward a Fault-Tolerant Star Tracker for Small Satellite Applications. *IEEE Trans. Aerosp. Electron. Syst.* **2020**, *56*, 3421–3431. [CrossRef]
3. Zhou, D.; Sheng, M.; Wang, Y.; Li, J.; Han, Z. Machine Learning-Based Resource Allocation in Satellite Networks Supporting Internet of Remote Things. *IEEE Trans. Wirel. Commun.* **2021**, *20*, 6606–6621. [CrossRef]
4. Zhu, Y.; Bai, W.; Sheng, M.; Li, J.; Zhou, D.; Han, Z. Traffic Allocation for Heterogeneous Links in Satellite Data Relay Networks. *IEEE Trans. Veh. Technol.* **2021**, *70*, 8065–8079. [CrossRef]
5. Liu, H.; Chu, Y.; Zhang, Y.; Hou, W.; Li, Y.; Yao, Y.; Cai, Y. Strategy of Multi-Beam Spot Allocation for GEO Data Relay Satellite Based on Modified K-Means Algorithm. *Mathematics* **2021**, *9*, 1718. [CrossRef]
6. Bi, Y.; Han, G.; Xu, S.; Wang, X.; Lin, C.; Yu, Z.; Sun, P. Software Defined Space-Terrestrial Integrated Networks: Architecture, Challenges, and Solutions. *IEEE Netw.* **2018**, *33*, 22–28. [CrossRef]
7. Chin, K.B.; Brandon, E.J.; Bugga, R.V.; Smart, M.C.; Jones, S.C.; Krause, F.C.; West, W.C.; Bolotin, G.G. Energy Storage Technologies for Small Satellite Applications. *Proc. IEEE* **2018**, *106*, 419–428. [CrossRef]
8. Zhou, D.; Sheng, M.; Li, B.; Li, J.; Han, Z. Distributionally Robust Planning for Data Delivery in Distributed Satellite Cluster Network. *IEEE Trans. Wirel. Commun.* **2019**, *18*, 3642–3657. [CrossRef]
9. Fraire, J.A.; Nies, G.; Gerstacker, C.; Hermanns, H.; Bay, K.; Bisgaard, M. Battery-Aware Contact Plan Design for LEO Satellite Constellations: The Ulloriaq Case Study. *IEEE Trans. Green Commun. Netw.* **2020**, *4*, 236–245. [CrossRef]
10. Yang, Y.; Xu, M.; Wang, D.; Wang, Y. Towards Energy-Efficient Routing in Satellite Networks. *IEEE J. Sel. Areas Commun.* **2016**, *34*, 3869–3886. [CrossRef]
11. Jiang, C.; Zhu, X. Reinforcement Learning Based Capacity Management in Multi-Layer Satellite Networks. *IEEE Trans. Wirel. Commun.* **2020**, *19*, 4685–4699. [CrossRef]

12. Dai, C.; Li, C.; Fu, S.; Zhao, J.; Chen, Q. Dynamic Scheduling for Emergency Tasks in Space Data Relay Network. *IEEE Trans. Veh. Technol.* **2021**, *70*, 795–807. [CrossRef]
13. Liu, R.; Sheng, M.; Xu, C.; Li, J.; Wang, X.; Zhou, D. Antenna Slewing Time Aware Mission Scheduling in Space Networks. *IEEE Commun. Lett.* **2017**, *21*, 516–519. [CrossRef]
14. Wang, L.; Jiang, C.; Kuang, L.; Wu, S.; Huang, H.; Qian, Y. High-Efficient Resource Allocation in Data Relay Satellite Systems With Users Behavior Coordination. *IEEE Trans. Veh. Technol.* **2018**, *67*, 12072–12085. [CrossRef]
15. Zhou, D.; Sheng, M.; Wang, X.; Xu, C.; Liu, R.; Li, J. Mission Aware Contact Plan Design in Resource-Limited Small Satellite Networks. *IEEE Trans. Commun.* **2017**, *65*, 2451–2466. [CrossRef]
16. Zhou, D.; Sheng, M.; Liu, R.; Wang, Y.; Li, J. Channel-Aware Mission Scheduling in Broadband Data Relay Satellite Networks. *IEEE J. Sel. Areas Commun.* **2018**, *36*, 1052–1064. [CrossRef]
17. Du, J.; Jiang, C.; Qian, Y.; Han, Z.; Ren, Y. Resource Allocation With Video Traffic Prediction in Cloud-Based Space Systems. *IEEE Trans. Multim.* **2016**, *18*, 820–830. [CrossRef]
18. Zhou, D.; Sheng, M.; Luo, J.; Liu, R.; Li, J.; Han, Z. Collaborative Data Scheduling With Joint Forward and Backward Induction in Small Satellite Networks. *IEEE Trans. Commun.* **2019**, *67*, 3443–3456. [CrossRef]
19. Deng, B.; Jiang, C.; Kuang, L.; Guo, S.; Lu, J.; Zhao, S. Two-Phase Task Scheduling in Data Relay Satellite Systems. *IEEE Trans. Veh. Technol.* **2018**, *67*, 1782–1793. [CrossRef]
20. He, L.; Li, J.; Sheng, M.; Liu, R.; Guo, K.; Zhou, D. Dynamic Scheduling of Hybrid Tasks With Time Windows in Data Relay Satellite Networks. *IEEE Trans. Veh. Technol.* **2019**, *68*, 4989–5004. [CrossRef]
21. Wang, L.; Jiang, C.; Kuang, L.; Wu, S.; Fei, L.; Huang, H. Mission Scheduling in Space Network with Antenna Dynamic Setup Times. *IEEE Trans. Aerosp. Electron. Syst.* **2019**, *55*, 31–45. [CrossRef]
22. Chen, X.; Li, X.; Wang, X.; Luo, Q.; Wu, G. Task Scheduling Method for Data Relay Satellite Network Considering Breakpoint Transmission. *IEEE Trans. Veh. Technol.* **2021**, *70*, 844–857. [CrossRef]
23. Wang, Y.; Sheng, M.; Li, J.; Wang, X.; Liu, R.; Zhou, D. Dynamic Contact Plan Design in Broadband Satellite Networks With Varying Contact Capacity. *IEEE Commun. Lett.* **2016**, *20*, 2410–2413. [CrossRef]
24. An, K.; Liang, T. Hybrid Satellite-Terrestrial Relay Networks With Adaptive Transmission. *IEEE Trans. Veh. Technol.* **2019**, *68*, 12448–12452. [CrossRef]
25. Deng, Z.; Yu, X.; Lin, W.; Wang, K.; Liu, H.; Gu, L.; Liu, Y.; Ma, X. A Multi-Beam Satellite Cooperative Transmission Scheme Based on Resources Optimization and Packets Segmentation. *Electronics* **2021**, *10*, 2841. [CrossRef]
26. Peng, C.; Wang, G.; Li, F.; Liu, H. Joint Resource Allocation for SWIPT-Based Two-Way Relay Networks. *Energies* **2020**, *13*, 6024. [CrossRef]
27. Han, S.; Li, L.; Li, X. Deep Q-Network-Based Cooperative Transmission Joint Strategy Optimization Algorithm for Energy Harvesting-Powered Underwater Acoustic Sensor Networks. *Sensors* **2020**, *20*, 6519. [CrossRef]
28. Chen, Z.; Xiao, N.; Han, D. Multilevel Task Offloading and Resource Optimization of Edge Computing Networks Considering UAV Relay and Green Energy. *Appl. Sci.* **2020**, *10*, 2592. [CrossRef]
29. Cheng, X.; Lyu, F.; Quan, W.; Zhou, C.; He, H.; Shi, W.; Shen, X. Space/Aerial-Assisted Computing Offloading for IoT Applications: A Learning-Based Approach. *IEEE J. Sel. Areas Commun.* **2019**, *37*, 1117–1129. [CrossRef]
30. Asuquo, P.M.; Cruickshank, H.S.; Ogah, C.P.A.; Lei, A.; Sun, Z. A Distributed Trust Management Scheme for Data Forwarding in Satellite DTN Emergency Communications. *IEEE J. Sel. Areas Commun.* **2018**, *36*, 246–256. [CrossRef]
31. Zhang, S.; Cui, G.; Wang, W. Joint Data Downloading and Resource Management for Small Satellite Cluster Networks. *IEEE Trans. Veh. Technol.* **2022**, *71*, 887–901. [CrossRef]
32. Fraire, J.A.; Madoery, P.G.; Finochietto, J.M.; Leguizamón, G. An evolutionary approach towards contact plan design for disruption-tolerant satellite networks. *Appl. Soft Comput.* **2017**, *52*, 446–456. [CrossRef]
33. Wan, Y.; Long, J.; Liu, L.; Qian, Z.; Zhong, S. Downlink aware data scheduling with delay guarantees in resource-limited leo satellite networks. *Peer-to-Peer Netw. Appl.* **2021**, *14*, 3291–3306. [CrossRef]
34. Fraire, J.A.; Madoery, P.G.; Charif, A.; Finochietto, J.M. On route table computation strategies in Delay-Tolerant Satellite Networks. *Ad Hoc Netw.* **2018**, *80*, 31–40. [CrossRef]
35. Zhang, T.; Li, H.; Zhang, S.; Li, J.; Shen, H. STAG-Based QoS Support Routing Strategy for Multiple Missions Over the Satellite Networks. *IEEE Trans. Commun.* **2019**, *67*, 6912–6924. [CrossRef]
36. Shi, K.; Zhang, X.; Zhang, S.; Li, H. Time-Expanded Graph Based Energy-Efficient Delay-Bounded Multicast Over Satellite Networks. *IEEE Trans. Veh. Technol.* **2020**, *69*, 10380–10384. [CrossRef]
37. Raverta, F.D.; Fraire, J.A.; Madoery, P.G.; Demasi, R.A.; Finochietto, J.M.; D'Argenio, P.R. Routing in Delay-Tolerant Networks under uncertain contact plans. *Ad Hoc Netw.* **2021**, *123*, 102663. [CrossRef]
38. Golkar, A.; i Cruz, I.L. The Federated Satellite Systems paradigm: Concept and business case evaluation. *Acta Astronaut.* **2015**, *111*, 230–248. [CrossRef]
39. Zheng, K.; Liu, F.; Zheng, Q.; Xiang, W.; Wang, W. A Graph-Based Cooperative Scheduling Scheme for Vehicular Networks. *IEEE Trans. Veh. Technol.* **2013**, *62*, 1450–1458. [CrossRef]
40. Nardin, A.; Fraire, J.A.; Dovis, F. Contact Plan Design for GNSS Constellations: A Case Study with Optical Intersatellite Links. *IEEE Trans. Aerosp. Electron. Syst.* **2022**, *58*, 1981–1995. [CrossRef]

41. Lu, C.; Liu, Q.; Zhang, B.; Yin, L. A Pareto-based hybrid iterated greedy algorithm for energy-efficient scheduling of distributed hybrid flowshop. *Expert Syst. Appl.* **2022**, *204*, 117555. [CrossRef]
42. Neely, M.J. Stochastic network optimization with application to communication and queueing systems. *Synth. Lect. Commun. Netw.* **2010**, *3*, 1–211.